I R A M P
8(2), December 2017, pp. 81-91

ISSN: 2229-3159

One and Two Photon Ionization along the Fe Isonuclear Sequence

M. S. PINDZOLA[1] AND J. P. COLGAN[2]

[1] *Department of Physics, Auburn University, Auburn, AL, USA*
[2] *Theoretical Division, Los Alamos National Laboratory, Los Alamos, NM, USA*

ABSTRACT: A time-dependent close-coupling method is used to calculate the one and two photon ionization cross sections along the *Fe* isonuclear sequence. Specific calculations are made for the ground configuration of Fe^{14+}, Fe^{15+}, Fe^{16+}, and Fe^{17+}. These calculations are in support of efforts to compare theory and experiment for iron opacities in hot dense plasmas.

1. INTRODUCTION

Recent measurements[1] of the iron opacity in hot dense plasmas are higher than those predicted by several theoretical opacity models [2, 3, 4, 5, 6, 7]. A possible explanation of the discrepancy is that the theoretical models did not include two-photon processes [8].

In this paper, we use a time-dependent close-coupling method to calculate one and two photon ionization along the *Fe* isonuclear sequence. Specific calculations are made for the ground configuration of Fe^{14+}, Fe^{15+}, Fe^{16+}, and Fe^{17+}. For single ionization we use a time-dependent close-coupling in three dimensions (TDCC-3D) method that has been used before for bare ion collisions with a one-active electron atom[9]. In the past we have used a time-dependent close-coupling in six dimensions (TDCC-6D) method to study both single and double ionization of He, Be, and Mg[10, 11].

The rest of the paper is organized as follows: in Section 2 we review the time-dependent close-coupling method, in Section 3 we calculate one and two photon ionization cross sections for Fe^{14+}, Fe^{15+}, Fe^{16+}, and Fe^{17+}, while in Section 4 we conclude with a brief summary. Unless otherwise stated, we will use atomic units.

2. THEORY

The time-dependent Schrodinger equation for a one active electron atom is given by:

$$i\frac{\partial\Psi(\vec{r},t)}{\partial t} = \left(-\frac{1}{2}\nabla^2 - \frac{Z}{r} + V(r)\right)\Psi(\vec{r},t) + E(t)\cos(\omega t)\, r\, \cos(\theta)\Psi(\vec{r},t), \tag{1}$$

where Z is the atomic number, $V(r)$ is the atomic potential produced by the inactive electrons, $E(t)$ is the electric field amplitude, and ω is the radiation field frequency. For the extraction of cross sections, a "constant" intensity pulse is chosen of the form:

$$E(t) = \begin{cases} E_0 \sin^2\left(\dfrac{\pi t}{2T}\right) & for\ t < T \\ E_0 & for\ T < t < (N-1)T \\ E_0 \sin^2\left(\pi t / 2(N-1)T\right) & for\ (N-1)T < t < NT \end{cases} \tag{2}$$

where $E_0 = (5.336 \times 10^{-9})\sqrt{I}, I$ is the intensity in W cm^{-2}, $T = 2\pi/\omega$ is a field period, and N is the number of field periods.

Expanding the total wavefunction, $\Psi(\vec{r},t)$, in spherical harmonics and substitution into Eq.(1) yields the time-dependent close-coupled equations:

$$i\frac{\partial P_l(r,t)}{\partial t} = T_l(r)\,P_l(r,t) + \Sigma_{l'} W_{ll'}(r,t)\,P_{l'}(r,t), \tag{3}$$

where

$$T_l(r) = -\frac{1}{2}\frac{d^2}{dr^2} + \frac{l(l+1)}{2r^2} - \frac{Z}{r} + V(r) \tag{4}$$

and

$$W_{ll'}(r,t) = E(t)\cos(\omega t)\, r\, \sqrt{(2l+1)(2l'+1)} \begin{pmatrix} l & 1 & l' \\ 0 & 0 & 0 \end{pmatrix}^2 \tag{5}$$

The atomic potential produced by the inactive electrons is approximated by:

$$V(r) = V_H(r) - \frac{\alpha_l}{2}\left(\frac{24\rho(r)}{\pi}\right)^{1/3}, \tag{6}$$

where $V_H(r)$ is the direct Hartree potential and $\rho(r)$ is the probability density in the local exchange potential. The bound radial orbitals needed to construct the atomic potential are calculated using a Hartree-Fock (HF) atomic structure code[12].

At time $t = 0$ the radial function is given by:

$$P_l(r, t=0) = \tilde{P}_{n_0 l_0}(r)\,\delta_{l,l_0}, \tag{7}$$

where bound, $\tilde{P}_{nl}(r)$, and continuum, $\tilde{P}_{kl}(r)$, radial wavefunctions are obtained by diagonalization of the Hamiltonian, $T_l(r)$, of Eq.(4). Following time propagation of the close-coupled equations of Eq.(3), momentum space probability amplitudes are calculated using:

$$K_l(k) = \int_0^\infty dr\, \tilde{P}_{kl}(t)\, P_l(r, t \to \infty) \tag{8}$$

The total probability for single ionization is given by:

$$\mathcal{P}_{single} = \int_0^\infty dk \sum_l |K_l(k)|^2 \tag{9}$$

The total generalized cross section for *n* photon single ionization is given by:

$$\sigma^n_{single} = \left(\frac{\omega}{I}\right)^n \frac{\mathcal{P}_{single}}{(N-1)T}. \tag{10}$$

3. RESULTS

The time-dependent close-coupling in three dimensions (TDCC-3D) method is used to calculate one and two photon single ionization cross sections for the ground configuration of Fe^{14+}, Fe^{15+}, Fe^{16+}, and Fe^{17+}. In all the calculations we employ a 480 point radial mesh with a uniform spacing of $\Delta r = 0.02$, an intensity $I = 10^{14}$ W cm^{-2}, and the number of field periods $N = 10$. Changes in the radial mesh, the intensity, and the number of field periods had very little effect on the final cross sections. We note that the TDCC-3D method does not yield a rapid turn-on at the various ionization thresholds. In addition, the TDCC-3D method does not map out narrow resonance structures, many of which take femto-seconds to decay.

3.1. Fe^{14+} $1s^22s^22p^63s^2$ ' $1s^22s^22p^63skl$ cross sections

Using core pseudopotentials for the 3*s* and 3*p* orbitals, bound and continuum orbitals for Fe^{14+} are found by repeated matrix diagonalizations of $T_l(r)$ of Eq. (4) while adjusting the parameter α_l in Eq.(6) to achieve agreement with Hartree-Fock semi-Relativistic (HFR) ionization potentials[13]. For $l = 0$ and $\alpha_0 = 0.73$ we obtained 8 bound states, with $\tilde{P}_{3s}(r)$ at -454 eV. For $l = 1$ and $\alpha_1 = 0.48$ we obtained 8 bound states, with $\tilde{P}_{3p}(r)$ at -422 eV. For $l = 2$ and $\alpha_2 = 0.37$ we obtained 8 bound states, with $\tilde{P}_{3d}(r)$ at -370 eV.

The TDCC-3D equations were then solved for the 3 coupled channels (l = 0,1,2) with the initial condition provided by Eq.(7) with $\tilde{P}_{3s}(r)$. One and two photon single ionization cross sections are presented in Figure 1.

We made calculations for one photon single ionization with a threshold of 454 eV, as seen in Figure 1a. A configuration-average distorted-wave (CADW) method[14] was used to calculate a cross section of 1.1×10^{-19} cm^2 at a photon energy of 500 eV, which is in reasonable agreement with the TDCC-3D results.

We made calculations for two photon single ionization with a threshold of 227 eV, as seen in Figure 1b. Using the HFR method, we calculated the excitation energies for the transition $3s^2 \rightarrow 3s4p$ to be at 233 eV and for the transition $3s^2 \rightarrow 3s5p$ to be at 317 eV. As seen in Figure 1b, the generalized cross section drops off from threshold to 260 eV followed by a slight rise and fall between 300 eV and 320 eV. Numerical results are given in Table 1.

3.2. Fe^{14+} $1s^22s^22p^63s^2 \rightarrow 1s^22s^22p^53s^2kl$ cross sections

Using a core pseudopotential for the 2*s* orbital, bound and continuum orbitals for Fe^{14+} are found by repeated matrix diagonalizations of $T_l(r)$ of Eq.(4) while adjusting the parameter α_l in Eq.(6) to achieve agreement with HFR ionization potentials[13]. For $l = 0$ and $\alpha_0 = 0.73$ we obtained 9 bound states, with $\tilde{P}_{3s}(r)$ at -454 eV. For $l = 1$ and $\alpha_1 = 1.01$ we obtained 9 bound states, with $\tilde{P}_{2p}(r)$ at -1176 eV. For $l = 2$ and $\alpha_2 = 0.37$ we obtained 8 bound states, with $\tilde{P}_{3d}(r)$ at -370 eV.

The TDCC-3D equations were then solved for the 4 coupled channels (l = 0,1,2,3) with the initial condition provided by Eq.(7) with $\tilde{P}_{2p}(r)$. One and two photon single ionization cross sections are presented in Figure 2.

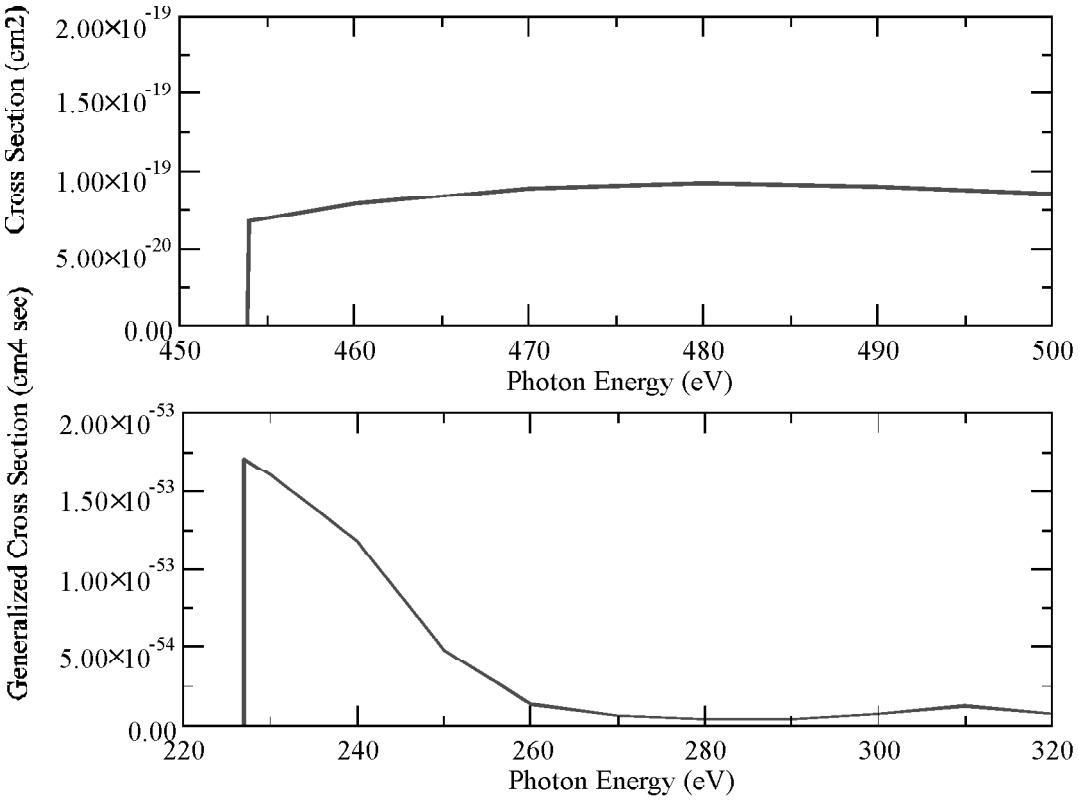

Figure 1: (color online) Fe^{14+} $1s^2 2s^2 2p^6 3s^2 \rightarrow 1s^2 2s^2 2p^6 3skl$ **ionization. Top graph: one photon absorption, Bottom graph: two photon absorption**

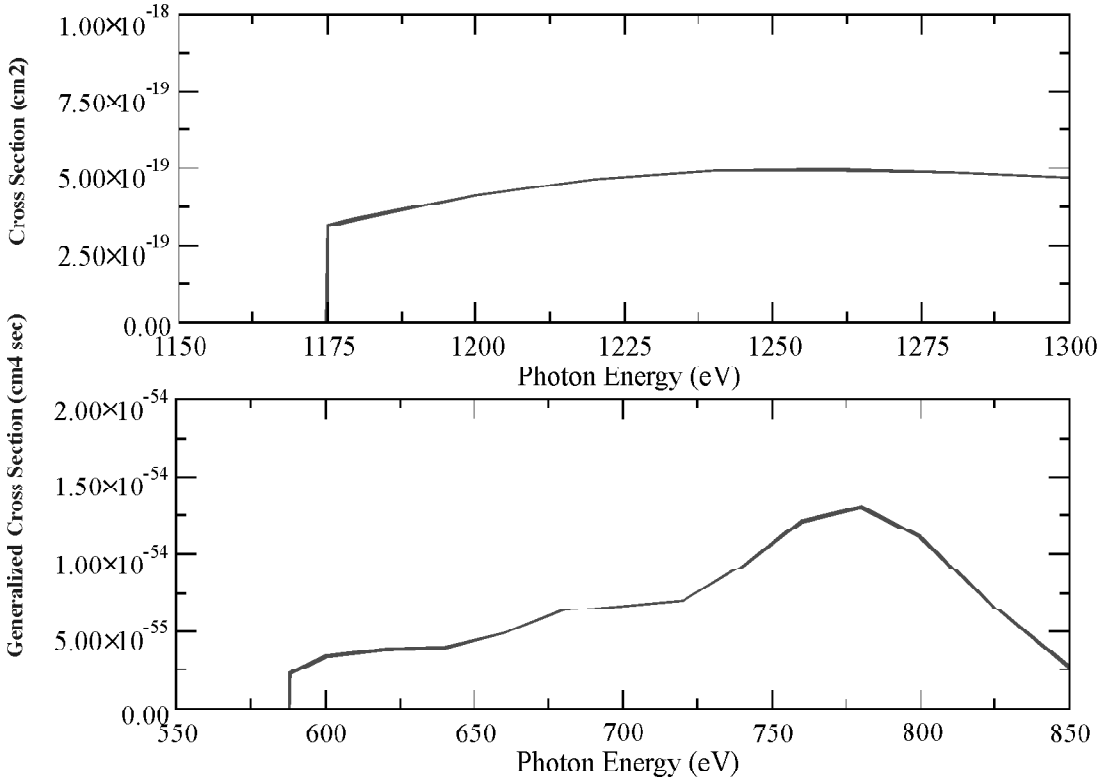

Figure 2: (color online) Fe^{14+} $1s^2 2s^2 2p^6 3s^2 \rightarrow 1s^2 2s^2 2p^5 3s^2\ kl$ **ionization. Top graph: one photon absorption, Bottom graph: two photon absorption**

We made calculations for one photon single ionization with a threshold of 1176 eV, as seen in Figure 2a. A configuration-average distorted-wave (CADW) method[14] was used to calculate a cross section of 3.4×10^{-19} cm^2 at a photon energy of 1300 eV, which is in reasonable agreement with the TDCC-3D results.

We made calculations for two photon single ionization with a threshold of 588 eV, as seen in Figure 2b. Using the HFR method, we calculated the excitation energies for the transition $2p^6 3s^2 \rightarrow 2p^5 3s^2 3p$ to be at 739 eV and for the transition $2p^6 3s^2 \rightarrow 2p^5 3s^2 3d$ to be at 792 eV. As seen in Figure 2b, there is a rise and then fall in the generalized cross section between 725 eV and 825 eV. Numerical results are given in Table 2.

Table 1
Two photon Fe^{14+} $1s^2 2s^2 2p^6 3s^2 \rightarrow 1s^2 2s^2 2p^6 3skl$ ionization

Photon Energy (eV)	*Generalized Cross Section (cm^4 sec)*
227	1.70E-53
230	1.60E-53
240	1.18E-53
250	4.82E-54
260	1.39E-54
270	6.44E-55
280	4.15E-55
290	4.14E-55
300	7.38E-55
310	1.25E-54
320	7.38E-55

Table 2
Two photon Fe^{14+} $1s^2 2s^2 2p^6 3s^2 \rightarrow 1s^2 2s^2 2p^5 3s^2 kl$ ionization

Photon Energy (eV)	*Generalized Cross Section (cm^4 sec)*
588	2.23E-55
590	2.44E-55
600	3.32E-55
620	3.82E-55
640	3.92E-55
660	4.88E-55
680	6.33E-55
700	6.65E-55
720	7.00E-55
740	9.22E-55
760	1.21E-54
780	1.30E-54
800	1.11E-54
825	6.55E-55
850	2.69E-55

3.3. Fe^{15+} $1s^2 2s^2 2p^6 3s \rightarrow 1s^2 2s^2 2p^6 kl$ *cross sections*

Using core pseudopotentials for the 3*s* and 3*p* orbitals, bound and continuum orbitals for Fe^{15+} are found by repeated matrix diagonalizations of $T_l(r)$ of Eq.(4) while adjusting the parameter α_l in Eq. (6) to achieve agreement with HFR ionization potentials[13]. For $l = 0$ and $\alpha_0 = 1.00$ we obtained 9 bound states, with $\tilde{P}_{3s}(r)$ at -490 eV. For $l = 1$ and $\alpha_1 = 0.42$ we obtained 9 bound states, with $\tilde{P}_{3p}(r)$ at -453 eV. For $l = 2$ and $\alpha_2 = 0.40$ we obtained 9 bound states, with $\tilde{P}_{3d}(r)$ at -406 eV.

The TDCC-3D equations were then solved for the 3 coupled channels (l = 0,1,2) with the initial condition provided by Eq. (7) with $\tilde{P}_{3s}(r)$. One and two photon single ionization cross sections are presented in Figure 3.

We made calculations for one photon single ionization with a threshold of 490 eV, as seen in Figure 3a. A CADW method[14] was used to calculate a cross section 5.2×10^{-20} cm^2 at a photon energy of 540 eV, which is in reasonable agreement with the TDCC-3D results.

We made calculations for two photon single ionization with a threshold of 245 eV, as seen in Figure 3b. Using the HFR method, we calculated the excitation energies for the transition $3s \rightarrow 4p$ to be at 247 eV and for the transition $3s \rightarrow 5p$ to be at 338 eV. As seen in Figure 3b, the generalized cross section exhibits a rapid rise at threshold and drop off to 280 eV and also a broad rise and fall between 310 eV and 350 eV. Numerical results are given in Table 3.

3.4. Fe^{15+} $1s^2 2s^2 2p^6 3s \rightarrow 1s^2 2s^2 2p^5 3skl$ *cross sections*

Using a core pseudopotential for the 2*s* orbital, bound and continuum orbitals for Fe^{15+} are found by repeated diagonalizations of $T_l(r)$ of Eq.(4) while adjusting the parameter α_l in Eq.(6) to achieve agreement with HFR ionization

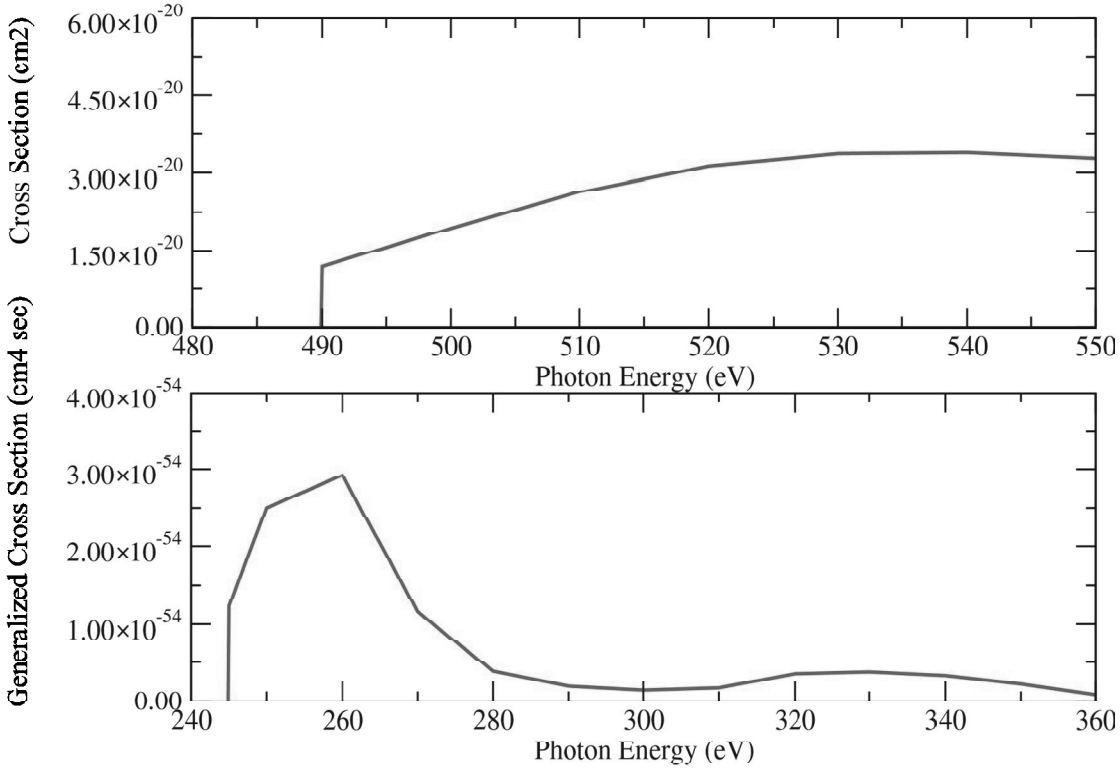

Figure 3: (color online) Fe^{15+} $1s^2 2s^2 2p^6 3s \rightarrow 1s^2 2s^2 2p^6$ kl **ionization. Top graph: one photon absorption, Bottom graph: two photon absorption**

Table 3
Two photon Fe^{15+} $1s^22s^22p^63s \rightarrow 1s^22s^22p^6kl$ ionization

Photon Energy (eV)	*Generalized Cross Section (cm^4 sec)*
245	1.23E-54
250	2.50E-54
260	2.92E-54
270	1.16E-54
280	3.84E-55
290	1.94E-55
300	1.44E-55
310	1.73E-55
320	3.50E-55
330	3.74E-55
340	3.27E-55
350	2.20E-55
360	8.67E-56

potentials[13]. For l = 0 and α_0 = 1.00 we obtained 10 bound states, with $\tilde{P}_{3s}(r)$ at -490 eV. For l = 1 and α_1 = 1.01 we obtained 10 bound states, with $\tilde{P}_{2p}(r)$ at -1220 eV. For l = 2 and α_2 = 0.40 we obtained 9 bound states, with $\tilde{P}_{3d}(r)$ at -406 eV.

The TDCC-3D equations were then solved for the 4 coupled channels (l = 0,1,2,3) with the initial condition provided by Eq.(7) with $\tilde{P}_{2p}(r)$. One and two photon single ionization cross sections are presented in Figure 4.

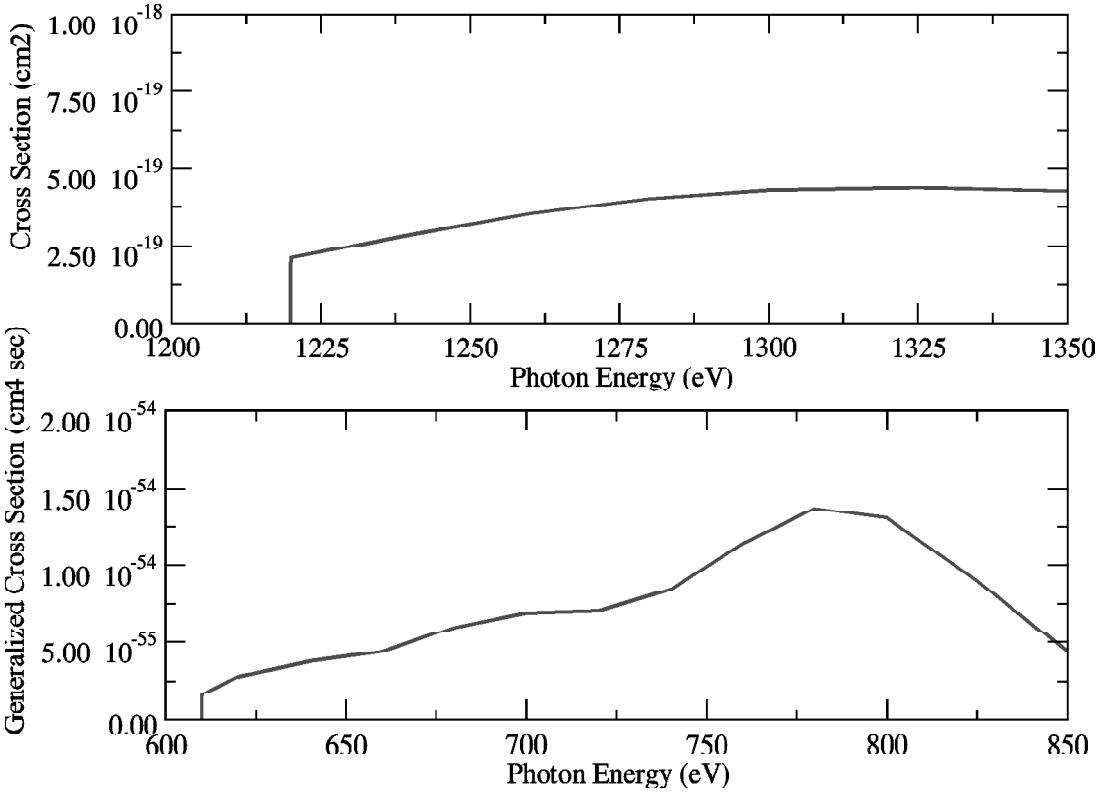

Figure 4: (color online) Fe^{15+} $1s^22s^22p^63s \rightarrow 1s^22s^22p^5\ 3skl$ ionization. Top graph: one photon absorption, Bottom graph: two photon absorption

We made calculations for one photon single ionization with a threshold of 1220 eV, as seen in Figure 4a. A CADW method[14] was used to calculate a cross section 3.5×10^{-19} cm^2 at a photon energy of 1280 eV, which is in reasonable agreement with the TDCC-3D results.

We made calculations for two photon single ionization with a threshold of 610 eV, as seen in Figure 4b. Using the HFR method, we calculated the excitation energies for the transition $2p^6 3s \rightarrow 2p^5 3s^2$ to be at 720 eV, for the transition $2p^6 3s \rightarrow 2p^5 3s 3p$ to be at 752 eV, and for the transition $2p^6 3s \rightarrow 2p^5 3s 3d$ to be at 801 eV. As seen in Figure 4b, there is a rise and then fall in the generalized cross section between 725 eV and 825 eV. Numerical results are given in Table 4.

Table 4
Two photon Fe^{15+} $1s^2 2s^2 2p^6 3s \rightarrow 1s^2 2s^2 2p^5 3skl$ ionization

Photon Energy (eV)	*Generalized Cross Section (cm^4 sec)*
610	1.66E-55
620	2.78E-55
640	3.76E-55
660	4.37E-55
680	5.98E-55
700	6.91E-55
720	7.07E-55
740	8.43E-55
760	1.14E-54
780	1.37E-54
800	1.31E-54
825	9.01E-55
850	4.44E-55

3.5. Fe^{16+} $1s^2 2s^2 2p^6 \rightarrow 1s^2 2s^2 2p^5 kl$ cross sections

Using a core pseudopotential for the 2*s* orbital, bound and continuum orbitals for Fe^{16+} are found by repeated matrix diagonalizations of $T_l(r)$ of Eq.(4) while adjusting the parameter α_l in Eq.(6) to achieve agreement with HFR ionization potentials[13]. For $l = 0$ and $\alpha_0 = 0.98$ we obtained 10 bound states, with $\tilde{P}_{3s}(r)$ at -536 eV. For $l = 1$ and $\alpha_1 = 0.49$ we obtained 10 bound states, with $\tilde{P}_{2p}(r)$ at -1266 eV. For $l = 2$ and $\alpha_2 = 0.40$ we obtained 9 bound states, with $\tilde{P}_{3d}(r)$ at -456 eV.

The TDCC-3D equations were then solved for the 4 coupled channels ($l = 0,1,2,3$) with the initial condition provided by Eq.(7) with $\tilde{P}_{2p}(r)$. One and two photon single ionization cross sections are presented in Figure 5.

We made calculations for one photon single ionization with a threshold of 1266 eV, as seen in Figure 5a. A CADW method[14] was used to calculate a cross section of 2.8×10^{-19} cm^2 at a photon energy of 1400 eV, which is in reasonable agreement with the TDCC-3D results.

We made calculations for two photon single ionization with a threshold of 633 eV, as seen in Figure 5b. Using the HFR method, we calculated the excitation energies for the transition $2p^6 \rightarrow 2p^5 3s$ to be at 730 eV and for the transition $2p^6 \rightarrow 2p^5 3d$ to be at 810 eV. As seen in Figure 5b, there is large rise and fall in the generalized cross section between 700 eV and 900 eV. Numerical results are given in Table 5.

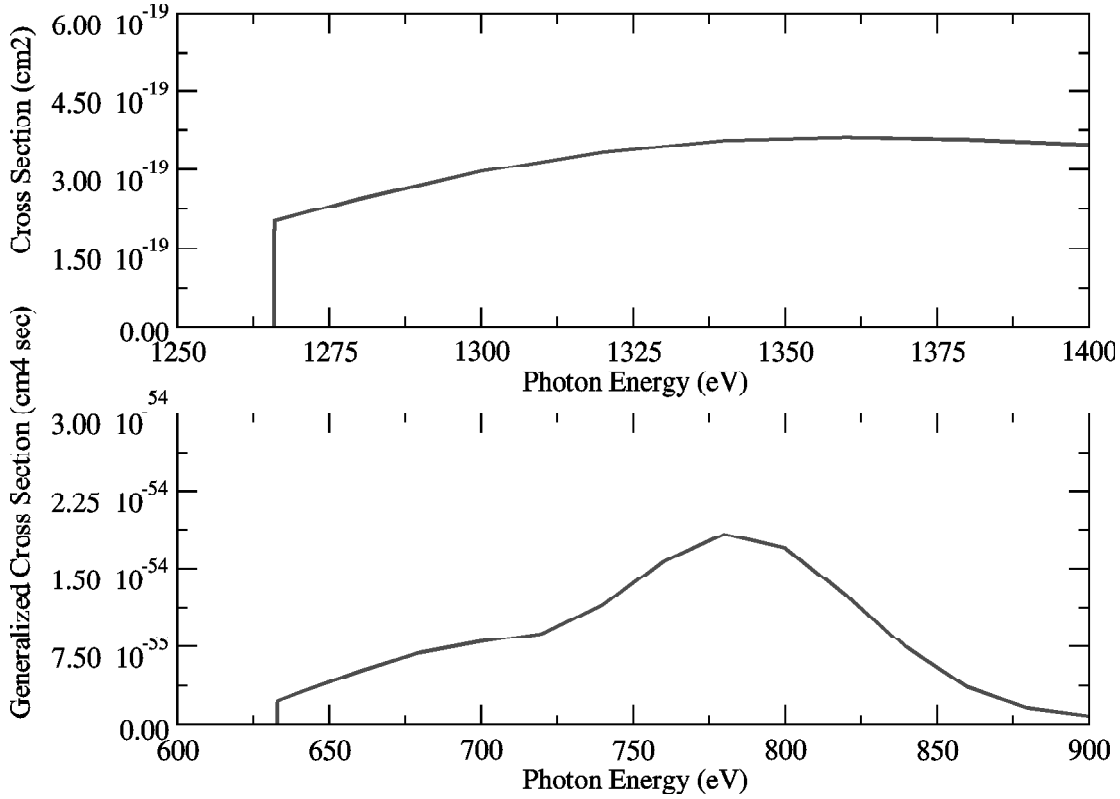

Figure 5: (color online) Fe^{16+} $1s^22s^22p^6 \rightarrow 1s^22s^22p^5kl$ **ionization. Top graph: one photon absorption, Bottom graph: two photon absorption**

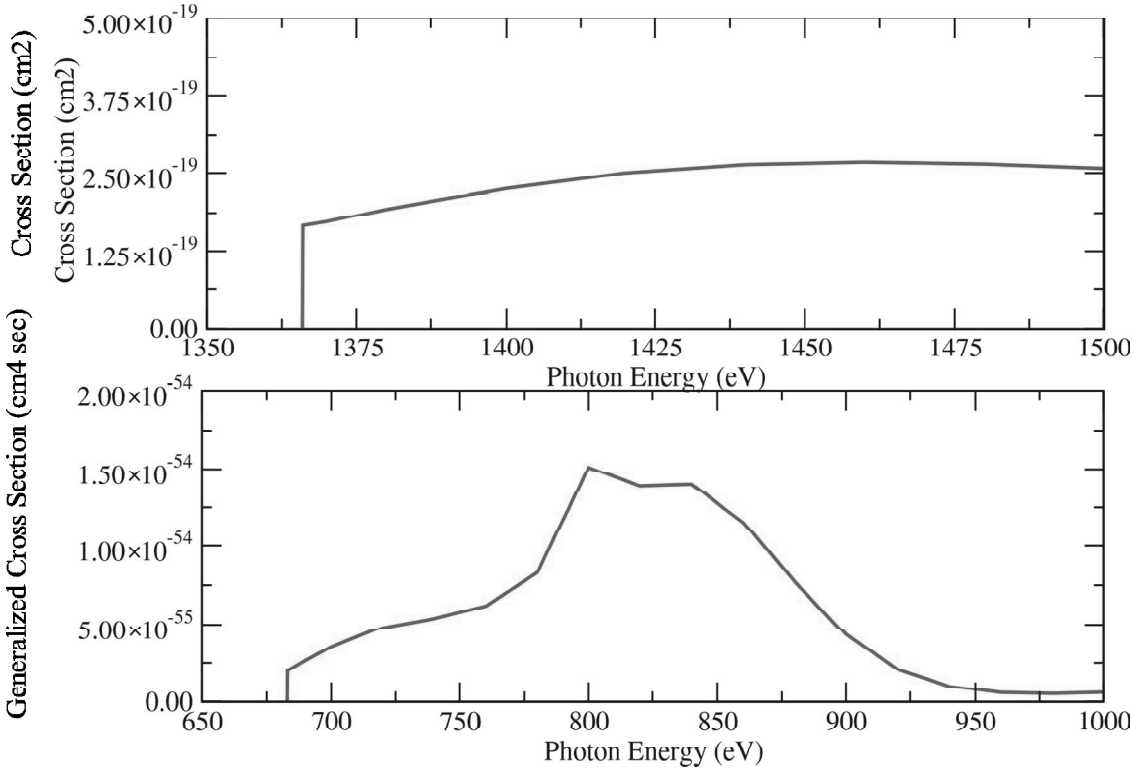

Figure 6: (color online) Fe^{17+} $1s^22s^22p^5 \rightarrow 1s^22s^22p^4kl$ **ionization. Top graph: one photon absorption, Bottom graph: two photon absorption**

Table 5
Two photon Fe^{16+} $1s^2 2s^2 2p^6 \rightarrow 1s^2 2s^2 2p^5 kl$ ionization

Photon Energy (EV)	*Generalized Cross Section (cm^4 sec)*
633	2.30E-55
635	2.51E-55
640	3.09E-55
660	5.15E-55
680	6.94E-55
700	7.97E-55
720	8.80E-55
740	1.15E-54
760	1.57E-54
780	1.83E-54
800	1.70E-54
820	1.25E-54
840	7.43E-55
860	3.66E-55
880	1.62E-55
900	8.58E-56

Table 6
Two photon Fe^{17+} $1s^2 2s^2 2p^5 \rightarrow 1s^2 2s^2 2p^4 kl$ ionization

Photon Energy (eV)	*Generalized Cross Section (cm^4 sec)*
683	2.01E-55
690	2.66E-55
700	3.52E-55
720	4.80E-55
740	5.39E-55
760	6.21E-55
780	8.29E-55
800	1.51E-54
820	1.39E-54
840	1.40E-54
860	1.15E-54
880	7.72E-55
900	4.32E-55
920	2.09E-55
940	9.80E-56
960	5.72E-56
980	5.09E-56
1000	5.83E-56

3.6. Fe^{17+} $1s^2 2s^2 2p^5 \rightarrow 1s^2 2s^2 2p^4 kl$ cross sections

Using a core pseudopotential for the 2*s* orbital, bound and continuum orbitals for Fe^{17+} are found by repeated matrix diagonalizations of $T_l(r)$ of Eq.(4) while adjusting the parameter α_l of Eq.(6) to achieve agreement with HFR ionization potentials[13]. For $l = 0$ and $\alpha_0 = 1.00$ we obtained 10 bound states, with $\tilde{P}_{3s}(r)$ at -584 eV. For $l = 1$ and $\alpha_1 = 0.48$ we obtained 10 bound states, with $\tilde{P}_{2p}(r)$ at -1366 eV. For $l = 2$ and $\alpha_2 = 0.36$ we obtained 9 bound states, with $\tilde{P}_{3d}(r)$ at -509 eV.

The TDCC-3D equations were then solved for the 4 coupled channels ($l = 0,1,2,3$) with the initial condition provided by Eq. (7) with $\tilde{P}_{2p}(r)$. One and two photon single ionization cross sections are presented in Figure 6.

We made calculations for one photon single ionization with a threshold of 1366 eV, as seen in Figure 6a. A CADW method[14] was used to calculate a cross section of 2.0×10^{-19} cm^2 at a photon energy of 1500 eV, which is in reasonable agreement with the TDCC-3D results.

We made calculations for two photon single ionization with a threshold of 683 eV, as seen in Figure 6b. Using the HFR method, we calculated the excitation energies for the transition $2p^5 \rightarrow 2p^4 3s$ to be at 783 eV and for the transition $2p^5 - 2p^4\ 3d$ to be at 858 eV. As seen in Figure 6b, there is a large rise and fall in the generalized cross section between 750 eV and 950 eV. Numerical results are given in Table 6.

4. SUMMARY

A time-dependent close-coupling method has been used to calculate the one and two photon ionization cross sections along the Fe isonuclear sequence. Specific calculations were made for the ground configuration of Fe^{14+}, Fe^{15+}, Fe^{16+}, and Fe^{17+}. The TDCC3D cross section results for one photon ionization were found to be in reasonable agreement with CADW results for all four Fe atomic ions. It is hoped that the TDCC3D generalized cross sections for two photon ionization presented in Tables 1-4 can be used in theoretical opacity models for Fe atomic ions in hot dense plasmas to compare with recent measurements[1].

Acknowledgments

This work was supported in part by grants from the US Department of Energy. Computational work was carried out at the National Energy Research Scientific Computing Center in Berkeley, California, and the High Performance Computing Center in Stuttgart, Germany.

References

[1] Bailey J E *et al*. 2015 Nature **517** 56

[2] Hansen S, Bauche J, Bauche-Arnoult C, and Gu M 2007 High Energy Density Physics **3** 109

[3] Seaton M J, Yu Y, Mihalas D, and Pradhan A K 1994 Mon. Not. R. Astron. Soc. **266** 805

[4] Badnell N R et al. 2005 Mon. Not. R. Astron. Soc. **360** 458

[5] Colgan J et al. 2013 High Energy Density Physics **9** 369

[6] Blancard C, Cosse P, and Faussurier G 2012 Astrophys. J. **745** 10

[7] Porcherot Q, Pain J C, Gilleron F, and Blenski T 2011 High Energy Density Physics **7** 234

[8] More R M, Hansen S B, and Nagayama T 2017 High Energy Density Physics **24** 44

[9] Pindzola M S, Colgan J, Robicheaux F, Lee T G, Ciappina M F, Foster M, Ludlow J A, and Abdel-Naby S A 2016 Advances in Atomic, Molecular, and Optical Physics **65** 291

[10] Colgan J and Pindzola M S 2002 Phys. Rev. Letts. **88** 173002

[11] Pindzola M S, Ballance C P, Abdel-Naby S A, Robicheaux F, Armstrong G S J, and Colgan J 2013 J. Phys. B **46** 035201

[12] Fischer C F 1987 Comput. Phys. Commun. **43** 355.

[13] Cowan R D 1981 *The Theory of Atomic Structure and Spectra*, University of California Press

[14] Pindzola M S, Ballance C P, Loch S D, Ludlow J A, Colgan J P, Witthoeft M C, and Kallman T R 2010 International Review of Atomic and Molecular Physics **1** No. 2 137.